Multi/Many-Objective Optimization Via A New Preference Indicator

1st Lianbo Ma
College of Software
Northeastern University
Shenyang, China
malb@swc.neu.edu.cn

2nd Mingli Shi
College of Software
Northeastern University
Shenyang, China
3053376397@qq.com

3rd Rui Wang
College of Software
Northeastern University
Shenyang, China
770439374@qq.com

4th ShengMinjie Chen
School of Mathematical Sciences
University of Chinese Academy of Sciences
Beijing, China
chenshengminjie19@mails.ucas.ac.cn

5th Junfei Zhao
2012 Laboratories
Huawei Technologies Co., Ltd.
Shenzhen, China
junfeng.zhao@huawei.com

6th Xiaolong Shen
2012 Laboratories
Huawei Technologies Co., Ltd.
Shenzhen, China
xiaolong3@huawei.com

***Abstract*—The development of preference-based optimizers has become an important trend in multi/many-objective optimization. Among those, the knees play a vital role in environmental selection process. Especially, they can accelerate convergence and maintain a high degree of diversity. Motivated by this, we suggest a new knees driven evolutionary algorithm based on pruning-power indicator to solve multi/many-objective problems. Here, the pruning power of a solution represents the number of points dominated by the solution in the local partition, which is used to identify knees. Then, an efficient pruning-power indicator is developed and then is proven mathematically to be able to characterize the solutions and further reduce the complexity of the hypervolume measurement. Based on this indicator, the algorithm uses angle-based partitioning and the nondominating sorting to accelerate convergence and maintain diversity of solutions. Finally, the algorithm is validated experimentally by using several DTLZ and WFG test problems and common performance measure. Experimental results validate the effectiveness of the proposed algorithm.**

***Index Terms*—Knees, preference, multi-objective optimization, many-objective optimization**

I. Introduction

Many real-world problems can be commonly considered as a multi-objective or many-objective optimization problem (MOP or MaOP) within which multiple objectives (more than 3 objectives refer to MaOP) are required to be optimized simultaneously and they are usually conflicted with each other. These MOPs can be found in many application areas, such as economics, engineering, and industrial networks [1]–[6]. Obviously, no single optimal solution that can satisfy all the objectives exists, but a set of trade-off solutions called Pareto optimal solutions (PS) can be obtained for MOPs. Accordingly, it is expected to obtain a set of all Pareto-optimal solutions called Pareto-optimal front (PF) [7], [8]. Recently, evolutionary algorithms (EAs) have become the popular approach to deal with MOPs and MaOPs since they have a strength of evolving individuals to approximate different sections of the PF simultaneously in a single run.. For these EAs, two main goals need to be considered: to minimize the distance of the population to the PF (i.e., convergence), and to maximize the spread of the population along the PF (i.e., diversity). A large number of multi-objective or many-objective EAs (MOEAs or MaOEAs) have been developed in the literatures based on the principle of different selection strategies, such as enhanced or relaxed dominance [8]–[11], decomposition with scalarizing aggregation functions [12], [13], performance indicators [14], [15] and hybrid approaches [16], [17]. It is worthy noted that in many MOEAs, the preferences are exploited deliberately to boost the algorithmic performance in terms of diversity and convergence of solutions. The preference information is used to govern population evolution towards the specific region of interest. For example, the solutions in the knee region of the PF will be naturally preferred if no other specific preferences. In KnEA [18], the knees are first identified based on the normal boundary intersection measure, and the density of the knee regions is adjusted by an adaptive niche strategy. This algorithm has been shown experimentally to be efficient for MaOPs. The KR-NSGA-II [19] utilizes the control of knee regions as mobile reference to guide the search process. In addition, if the reference vectors in MOEA/D can be considered as a kind of preferences [4], they have shown the merit of guiding the evolution of nondominated population towards the PF with desired diversity of population. Obviously, the use of preferences with other traditional multi-objective approaches can provide further insights on the characteristics of the obtained solutions.

In this paper, we suggest a new optimizer based on a new dominance preference for MOPs and MaOPs. First, the populations are mapped into a set of partitions in the form of

This work is supported by the National Natural Science Foundation of China under Grant No. 61773103, Fundamental Research Funds for the Central Universities No. N180408019 and Huawei HIRP project under Grant No. HO2019085002.

978-1-7281-6929-3/20/$31.00 ©2020 IEEE

hyperspherical coordinates. Then, the pruning power of each solution is evaluated to represent its dominance power over other members in their located partition. Usually, the solutions with better pruning power are preferred in the environmental selection because they can make more contribution to the search performance. Accordingly, the solutions in these partitions can be evolved independently towards the PF with more and more accurate approximation [18], [19].

In the proposed approach, the pruning power rate (PPR) indicator is used to approximate the localized hypervolume value within a local partition, which is conductive to enhancing convergence in multi-objective space. In addition, the solutions are regarded to evolve within different partitions rather than along different reference vectors. Based on the PPR indicator, the best pruning power points driven EA called BppEA is developed, where the individuals are mapped into the hyperspherical coordinates system, and the space is divided into a set of partitions. In principle, the best solutions in each partition are selected to approximate the PF based on PPR indicator, and this approximation will be more and more accurate with good diversity as the evolution proceeds.

The main contributions of this paper can be summarized as follows: The pruning power rate (PPR) evaluation method is proposed mathematically as a new performance indicator, which is useful to identify knees in the local part. Compared to conventional methods based on Euclidean distance, the PPR indicator is rather simple and effective, only using hyperspherical cooperates of solutions to the partition, which is more cost-efficient for many-objective optimization. In the hyperspherical partitioning approach, each partition not only specifies a unique subregion in the objective space, but also defines the positions of solutions in hyperspherical coordinates, which can enhance the diversity of population.

The remainder of this paper is organized as follows. In Section II, we give the design of of pruning power indicator. Then, the proposed algorithm are presented in Section III. Section IV gives the experimental study. Finally, conclusions are output in Section V.

II. Pruning Power Indicator

In this section, we aim to estimate the hypervolume dominated by a given point *p* in its located partition, defined as the pruning power rate of *p*.

In order to design the pruning power rate (PPR) criterion, we first give two basic definitions:

Definition 1 (pruning area): $\exists x \in p_i$ and p_i is the ith partition if condition: $S = \{y | x \succ y, \forall y \in p_i\}$, then the pruning area of x, i.e., $Darea(x)$, is defined as the volume of the hypercube constructed by S, i.e., $Darea(x) = V(S)$.

Definition 2 (pruning power rate): $\forall p_i$, $\exists x \in p_i$, if conditions satisfy: (i) $Area(p_i)$ is the volume of the partition hypercube covered by p_i, (ii) $Darea(x)$ is the pruning area of x, then the PPR of x is defined as $PPR(x) = \frac{Darea(x)}{Area(x)}$.

Then, we show how to calculate PPR in a conventional way. For bi-objective minimization problem, K partitions are preset by one angular dimension φ, given a solution $p = \{x_p, y_p\}$ in the ith partition, as shown in Fig.1, its PPR is calculated as

$$PPR(p) = \frac{Darea(x_p, y_p, \varphi_1, \varphi_2)}{Parea(\varphi_1, \varphi_2)} \tag{1}$$

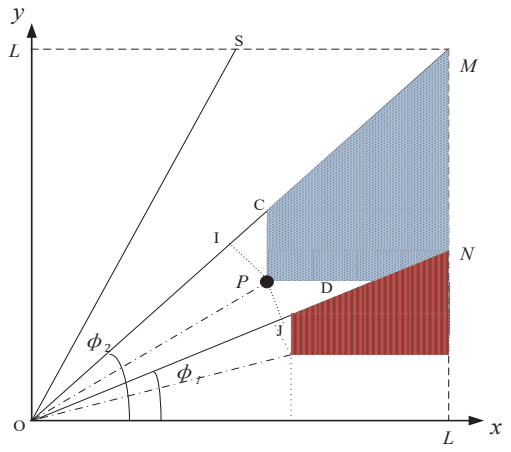

Fig. 1. Illustrating the main idea for calculating $PPR(P)$

From Fig.1, it is clear that $y_p = x_p tan\varphi_p$ where $0 \leqslant \varphi^{i-1} \leqslant \varphi^p \leqslant \varphi^i \leqslant \Pi/2$. For simplicity, we take the notation $\varphi_1 = \varphi^{i-1}$ and $\varphi_2 = \varphi^i$. As presented in [20], the pruning area of p is $Darea(x_p, y_p, \varphi_1, \varphi_2) = Area(\varphi_1, \varphi_2) - S_{OPC} - S_{OPD}$. Then, through the mathematical deductions, the pruning area of p where $0 \leqslant \varphi_1 \leqslant \varphi_2 \leqslant \Pi/4$ is calculated as

$$\begin{aligned} Darea(x_p, y_p, \varphi_1, \varphi_2) = Area(\varphi_1, \varphi_2) - \\ \frac{1}{2} * r_p * sin(\varphi_p - \varphi_1) * \frac{r_p * sin\varphi_p}{sin\varphi_1} - \\ \frac{1}{2} * r_p * sin(\varphi_2 - \varphi_p) * \frac{r_p * cos\varphi_p}{cos\varphi_2} \end{aligned} \tag{2}$$

Considering the symmetry and analogy of the case $\Pi/4 \leqslant \varphi_1 \leqslant \varphi_2 \leqslant \Pi/2$, the total area and pruning area are defined as

$$\begin{aligned} Area(\varphi_1, \varphi_2) = \frac{L^2}{2}(2 - tan\varphi_1 - \frac{1}{tan\varphi_2}) \\ Parea(x_p, y_p, \varphi_1, \varphi_2) = \\ Parea(x_p, y_p, \frac{\Pi}{2} - \varphi_1, \frac{\Pi}{2} - \varphi_2) \end{aligned} \tag{3}$$

Nevertheless, it is difficult to calculate in high dimensions. Thus, the equation of the PPR indicator can be further simplified as:

$$PPR'(X_p) = (sin(\varphi_2 - \varphi_p) + sin(\varphi_p - \varphi_1))/r \tag{4}$$

The detailed derivation process about PPR and PPR' is provided in the supplementary material[1]. The Pearson correlation coefficient (PCC) is used to validate the linear correlation

[1] https://github.com/NEU-EA/CEC2020

between PPR' and PPR in 9-partitioning case (as shown Fig.3 in [20]). Due to the space symmetry at $y = x$ (except for $\frac{y_p}{tan\varphi_1} = L$), we only consider the lower left partitions. Then, we select 10000 points randomly and record statistical results in Table 1. From this table, we can observe that PPR' strongly even extreme strongly correlates to PPR, and the identification accuracy of PPR' reaches more than 0.9.

TABLE I
CORRELATION AND ACCURACY OF THE REDUCED PPR

Partition	mean	median	min	max	std	PPR coeff
First partition	0.98	1	0.78	1	0.057	0.87
Second partition	0.98	1	0.84	1	0.043	0.94
Third partition	0.99	1	0.87	1	0.033	0.93

III. PROPOSED ALGORITHM

In this section. the best pruning power points driven EA (BppEA) is presented based on the pruning power indicator in detail, which is inspired on the nondominated sorting approach. The framework of BppEA is given in Algorithm 1.The main procedures of the algorithm are presented as follows.

Algorithm 1 Main framework of BppEA.

Input: N (population size), Max_Gen (the maximum number of generations)
Output: P (final population)
1: /* Initialization */
2: Generate the initial population P_t
3: /*n is the number of partitions*/
4: Angle_Boundary = Equi_volume_Partition(n)
5: /* Main Loop */
6: **while** $t \leq Max\_Gen$ **do**
7: Q_t = Variation(P_t)+ Mating selection(P_t)
8: $S_t = P_t \cup Q_t$
9: Multi-scale normalization S_t
10: /* Nondominated sort at i partion */
11: Nondominated_sort(S_t, Angle_Boundary)
12: K = Compute_pruning_power_of_points (S_t, Angle_Boundary)
13: P_t = Environmental_selection(S_t, K, N)
14: $t++$
15: **end while**

A. Hyperspherical space partitioning

The main goal of hyperspherical space partitioning is to divide the objective space into a set of partitions only by using the angular coordinates. There are two ways to generate these partitions. The equi-volume partitioning approach proposed in [20] uses angular coordinates to generate a set of equi-volume partitions. In addition, the reference vectors introduced in [12] can also be used to construct partitions: each reference vector is initialized as the center axis of each corresponding partition. In this paper, we use the first approach and its main procedures are as follows. First, the cartesian coordinates of the space is transformed to the hyperspherical coordinate system. And then, the following operations are performed according to [20]: suppose N is the number of partitions, S is the m-dimensional space, $S_i = \left[\varphi_1^{i-1}, \varphi_1^i\right] \times ... \times \left[\varphi_{m-1}^{i-1}, \varphi_{m-1}^i\right]$ where φ_j^{i-1} and φ_j^i are the boundary angular coordinates of φ_j in the partition i, and V_m is the total volume of S, in order to yield several approximately equant partitions, the volume of each partition is set to V_m/N, and the V_m^i for the ith partition is calculated as

$$V_m^i = \int_0^r \int_{\varphi_1^j}^{\varphi_1^{j+1}} ... \int_{\varphi_{m-1}^j}^{\varphi_{m-1}^{j+1}} dV \tag{5}$$

where dV is the volume element of the ith partition. And each of the angular coordinates $\varphi_1, \varphi_2, ..., \varphi_{m-1}$ is determined according to the condition$V_m^i = V_m/N$. The details can be referred to [20].

The following operation is to determine the boundaries of each partition for the fairness of the partitioning. As suggested in [20], we adopt a binary search approach to find the boundary angular coordinates. This search is based on the assumption that each angle φ_i is divided into $k = \sqrt[m-1]{N}$ parts, which ensures there are totally N partitions and $k-1$ boundary angles in the objective space. For example in the case with $m = 3$ and $N = 9$, the objective space can be divided into 3 parts by using φ_1 and φ_2, while $\varphi_1^1 = 48.21$, $\varphi_1^2 = 70.55$, $\varphi_2^1 = 30$ and $\varphi_2^2 = 60$.

B. Multi-scale normalization

The normalization is used to ensure all normalized individuals are located in the first quadrant of the coordinate system, without distorting their relative relationships on different-scale objectives. Here the Schur product is employed using the ideal point Z^* and the nadir point Z^{nad}, as

$$F_i(x) = \frac{f_i^{'}(x) \circ (z^{nad} - z^*)}{\left\| f_i^{'}(x) \circ (z^{nad} - z^*) \right\|} \tag{6}$$

where $f_i^{'}(x)$ is the ith translated objective value, $\circ$ denotes the Schur product and it takes two matrices of the same dimensions and produces another matrix, where each element is the product of elements of the original two matrices.

C. Compute_pruning_power_of_points

In principle, compute_purning_power_of_points aims to select the best points in terms of the pruning power, and add them to the population. The main steps include: (1) calculate the pruning power values of each solution in each partition, and (2) select a certain number of points with better pruning values to add them in the population one by one.

Due to that the pruning power of each point is evaluated in the form of hyperspherical coordinates, the diversity and convergence of solutions in the space can be easily managed according to its radial coordinate and angular coordinates.

Algorithm 2 Environmental_selection(P, K, N).

Input: P(Normalized population) K(Rank of Normalized population) N(Number of population)
Output: P_t(Offspring population)

$i = 0, id = 0$
$P_t = \emptyset, remain = \emptyset, n = length(K)$
$F = NDSort(P)$ // nondominated sorting
$P_t = P_t \cup F_1, i = i + |F_1|$
while $id \leq n$ and $i \leq N$ **do**
  $j = 0$
  $id++$
  while $j \leq (N - |F_1|)/n$ and $K_{id} \neq \emptyset$ **do**
    $P_t = P_t \cup (S : argmax_{S \in K_{id}} PP(s))$
    $K_{id} = K_{id} \backslash S$
    $j++$
    $i++$
  end while
  if $j \neq (N - |F_1|)/n$ **then**
    $remain = remain \cup (id, R = (N - |F_1|)/n - j)$
  end if
end while
while $remain \neq \emptyset$ and $i \leq N$ **do**
  $I(id, R_I) = \{I : I \in remain\}$
  $adj = \{K_{adjacent\_I}\}$
  $P_t = P_t \cup (S : random(adj, R_I))$
  $i = i + R_I$
  $K_{adjacent\_I} = K_{adjacent\_I} \backslash S$
end while

D. Environmental Selection

Environmental selection is to select better solutions as parents for the next generation. Similar to NSGA-II [7], these elitist solutions are selected from a combination of the parent and offspring populations. The non-dominated solutions in the parent population are selected firstly. Then, the pruning power evaluation PPR indicator is used in environmental selection. Algorithm 2 presents the main steps of environmental selection.

Note that before environmental selection, the normalized population is grouped into a set of partitions, and then the first $(N - |F_1|)/n$ best individuals are selected from the subpopulation for the next generation. However, there may not be enough individuals to be selected in some portions. In this case, unselected points in the adjacent partitions will be selected.

E. Time Complexity Analysis

Within a generation, for a population size N and an M-dimensional problem, the complexity of mating selection is $O(MN^2)$, and the simulated binary crossover (SBX) and polynomial mutation need computation time $O(DN)$ to generate N offspring, where D is the number of decision variables. In environmental selection, nondominated sorting needs computation time $O(MN^2)$, objective partitioning and PPR calculation need computation time $O(MN^2)$. To sum up, the time complexity of BppEA is $O(MN^2)$.

TABLE II
SETTING OF EXTERNAL AND INTERNAL DIVISIONS.

Objectives (m)	Divisions (H_1,H_2)	Weighted vectors (N)
3	12,0	91
5	6,0	210
8	3,2	156

TABLE III
PARAMETER SETTING OF T ON DTLZS AND WFGS.

Problem	Obj.3	Obj.5	Obj.8
DTLZ1	0.6	0.2	0.1
DTLZ2	0.6	0.2	0.1
DTLZ4	0.6	0.2	0.1
WFG1	0.5	0.5	0.5
WFG2	0.5	0.5	0.5

IV. EXPERIMENTAL RESULTS AND DISCUSSION

In this section, The BppEA is evaluated experimentally against NSGA-III [11], MOEA/D [12] and KnEA [18] on a set of benchmark functions. NSGA-III uses a set of uniform distributed reference points to promote the maintenance of population diversity based on NSGA-II [11]. MOEA/D is a decomposition-based EA [12]. The main idea of KnEA is to make use of knee points to enhance the search performance of MOEAs for MaOPs [18]. In KnEA, knee points among the non-dominated solutions are preferred in mating selection and environmental selection. Two widely used test bed suites, namely DTLZ and WFG, are used. The experiments are conducted on 5 test problems: DTLZ1, DTLZ2, DTLZ4, WFG1 and WFG2. And 3, 5 and 8 objectives will be respectively considered for each test problem.

A. Experimental Setting

All the compared algorithms have two common parameters: the maximum iteration number $MaxI$ and the population size N. Here $MaxI$ is 500 and N is set to 100. In addition, each algorithm is implemented 20 times independently on each problem. Other parameters for NSGA-III, MOEA/D and KnEA remain the same with their original references [11], [12], [18]. To be specific, the weight vectors of NSGA-III and MOEA/D are generated using a two layer scheme, as shown in Table II, where the settings of the external and internal divisions ($H1$ and $H2$) for different numbers of objectives are listed. According to [18], Table III gives the setting of the adjustable parameter T on DTLZ and WFG test suites for KnEA. As shown in Table III, T is set to 0.5 for DTLZ2, DTLZ4, and all test problems in the WFG suite.

For BppEA, several parameters are set empirically as: the population size is 120, and the number of partitions are set to 100,81 and 128 for the problems with 3, 5 and 8 objectives, respectively. As for the variation operator, BppEA use SBX

TABLE IV
IGD RESULTS OF COMPARED ALGORITHMS ON TEST SUITS, WHERE THE BEST TERMS ARE BOLD

Problem	Obj.	KnEA	MOEA/D	NSGA-III	BppEA
DTLZ1	3	2.2860E-02(2.87E-03)	3.1127E-02(6.59E-06)	2.0570E-02(1.33E-05)	**2.0141e-02(2.87e-04)**
	5	8.3830E-02(9.03E-04)	6.8067E-02(5.68E-06)	4.4044E-02(2.40E-01)	**4.1105e-02(1.60e-03)**
	8	2.7300E-01(4.19E-02)	**1.3770E-01(2.73E-04)**	1.4871E-01(2.40E-01)	1.5538e-01(1.52e-02)
DTLZ2	3	5.6420E-02(3.35E-02)	5.5464E-02(9.45E-08)	5.4957E-02(7.06E-05)	**5.4592e-02(1.92e-03)**
	5	**1.1460E-01(2.49E-03)**	2.1200E-01(8.33E-05)	2.1636E-01(8.28E-04)	2.1654e-01(1.82e-03)
	8	**2.5760E-01(2.58E-01)**	3.8680E-01(2.13E-05)	4.3354E-01(7.33E-02)	3.9164e-01(8.22e-04)
DTLZ4	3	**5.4230E-02(2.99E-03)**	5.4880E-02(2.18E-03)	5.4505E-02(4.95E-05)	5.7292e-02(1.21e-03)
	5	2.1670E-01(6.09E-05)	4.2682E-01(1.77E-04)	3.9178E-01(1.83E-01)	**2.1381e-01(4.80e-04)**
	8	**3.5280E-01(1.68E-02)**	4.8315E-01(9.56E-02)	4.7071E-01(1.15E-01)	3.9522e-01(6.34e-03)
WFG1	3	1.4130E+00(2.04E-01)	2.9978E-01(3.94E-03)	**1.4517E-01(1.50E-03)**	5.2736e-01(6.07e-02)
	5	2.2430E+00(4.21E-01)	1.2328E+00(6.26E-03)	5.0456E-01(8.06E-03)	**4.9828e-01(4.91e-02)**
	8	3.8110E+00(4.21E-01)	2.1185E+00(4.78E-02)	**1.1667E+00(5.84E-02)**	1.3317e+00(1.07e-01)
WFG2	3	2.3970E-01(1.33E-03)	7.3140E-01(2.16E-01)	1.8901E-01(5.19E-03)	**1.7006e-01(2.28e-02)**
	5	5.2450E-01(9.87E-02)	5.1584E+00(3.02E-02)	8.2326E-01(5.04E-03)	**4.7637e-01(2.24e-02)**
	8	2.6150E+00(2.12E-02)	8.6599E+00(1.84E-02)	3.3279E+00(1.14E+00)	**1.9417e+00(8.73e-02)**

crossover and polynomial mutation, with the distribution exponents $\eta_c = 20$ and $\eta_m = 20$, respectively. Crossover rate is $p_c = 1.0$, and mutation rate per variable is $p_m = 1/D$, where D is the number of decision variables.

B. Results And Analysis

The statistical results including the mean and standard deviation values in terms of the IGD metric obtained by the four MaOEAs are shown in Table IV, where the best items are highlighted. Generally, it is found that BppEA performs very competitively to other peer algorithms on DTLZ test instances, while NSGA-III also shows its superiority on DTLZ2.

To be specific, from Table IV, it can be observed that BppEA is able to find the best IGD values on all the problem instances of DTLZ1, DTLZ4, and WFG2. Both BppEA and NSGA-III perform powerfully on all test problems with 3 objectives. It is stressed that BppEA outperforms other algorithms on DTLZ1, and DTLZ4 when the number of objectives is larger than 5. Similar to that of KnEA and NSGA-III, the performance of BppEA is also very promising on the three DTLZ test problems with more than 3 objectives. Note that NSGA-III obtains the second best results on all the DTLZ problems, which shows its stale performance. Fig.2(a) and Fig.2(b) illustrate the evolution processes of IGD values obtained by BppEA on WFG2 with 3 and 8 objective, respectively. From these figures, it can be observed that as the number of objectives increases, BppEA becomes better in terms of the convergence and diversity.

From Table IV, we also see that MOEA/D and NSGA-III can obtain satisfactory results in terms of IGD on WFG problems with 3 or 5 objectives. From these experimental results, it is confirmed that MOEA/D and NSGA-III are competent algorithms for MaOPs with a small number of objectives. The performance of KnEA and BppEA is also encouraging since they are able to obtain comparable results with those of MOEA/D and NSGA-III on all WFG problems with more than 5 objectives. Furthermore, BppEA performs relatively better than NSGA-III and KnEA on WFG test problems with more than 3 objectives.

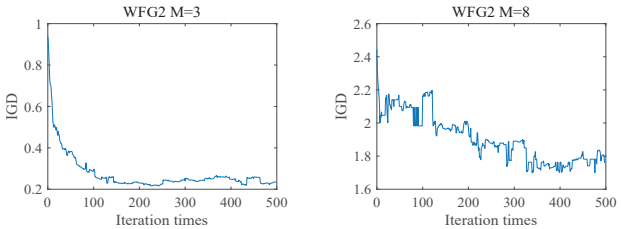

(a) 3-objective (b) 3-objective

Fig. 2. IGD values on WFG2 of BppEA

V. CONCLUSION

This paper develops a new MaOEA based on a new pruning power indicator called BppEA to solve MaOPs. BppEA aims to obtain excellent wideness and uniformity of solutions via enhancing environmental selection procedures with different evolution rules. Specifically, in BppEA, the search space is first split into a set of partitions in hyperspherical coordinate system, and then the pruning power (PPR) indicator is proposed to evaluate the dominance ability of each solution in the partition. At each generation, the solutions with best PPR values in each partition are expected to approximate different segments of the PF. In this way, the convergence and diversity of solutions can be maintained during the search process. The proposed algorithm has been experimentally test on a set of test benchmarks. Experimental results validate the effectiveness of the proposed approach. A comprehensive sensitivity analysis of parameters of the algorithm, and its real world applications will be highlighted in our future work.

ACKNOWLEDGMENT

This work is supported by the National Natural Science Foundation of China under Grant No. 61773103, and Huawei HIRP project under Grant No. HO2019085002.

REFERENCES

[1] J. G. Herrero, A. Berlanga, and J. M. M. Lpez, Effective evolutionary algorithms for many-specifications attainment: Application to air traf-

fic control tracking filters, IEEE Trans. Evol. Comput., vol. 13, no. 1, pp. 151C168, Feb. 2009.
[2] H. Ishibuchi and T. Murata, A multi-objective genetic local search algorithm and its application to flowshop scheduling, IEEE Trans. Syst., Man, Cybern. C, Appl. Rev., vol. 28, no. 3, pp. 392C403, Aug. 1998.
[3] L.Ma,R.Wang,M.Chen,W.Wang,S.Cheng,Y.Shi, A Novel Many-objective Evolution-ary Algorithm Based on Transfer Learning with Kriging model, Information Sciences,Vol. 509, 2020, pp. 437-456.
[4] J. Handl, D. B. Kell, and J. Knowles, Multiobjective optimization in bioinformatics and computational biology, IEEE/ACM Trans. Comput. Biol. Bioinformat., vol. 4, no. 2, pp. 279C292, Apr. 2007.
[5] A. Ponsich, A. L. Jaimes, and C. A. C. Coello, A survey on multiobjective evolution-ary algorithms for the solution of the portfolio optimization problem and other finance and economics applications, IEEE Trans. Evol. Comput., vol. 17, no. 3, pp. 321C344, Jun. 2013.
[6] L. Ma, X. Wang, M.Huang, Z.Lin, L..Tian, H.Chen. Two-level Master-slave RFID Networks Planning via Hybrid Multi-objective Artificial Bee Colony Optimizer, IEEE Transactions on Systems, Man, and Cybernetics: Systems, PP(99):1-20. 2017.
[7] K. Deb, A. Pratap, S. Agarwal, and T. Meyarivan, A fast and elitist multi-objective ge-netic algorithm: NSGA-II, IEEE Trans. Evol. Comput., vol. 6, no. 2, pp. 182C197, Apr. 2002.
[8] Y. Yuan, H. Xu, B. Wang, and X. Yao, A new dominance relation based evolutionary algorithm for many-objective optimization, IEEE Trans. Evol. Comput., vol. 20, no. 1, pp. 16C37, 2016.
[9] M. Koppen and K. Yoshida, Substitute distance assignments in NSGAII for handling many-objective optimization problems, in Proc. Evol. Multi-Criterion Optimization, 2007, pp. 727C741.
[10] S. Yang, M. Li, X. Liu, and J. Zheng, A grid-based evolutionary algorithm for many-objective optimization, IEEE Trans. Evol. Comput., vol. 17, no. 5, pp. 721C736, Oct. 2013.
[11] K. Deb and H. Jain, An evolutionary many-objective optimization algorithm using ref-erence-point based non-dominated sorting approach, part I: Solving problems with box con-straints, IEEE Trans. Evol. Comput., vol. 18, no. 4, pp. 577C601, Sep. 2014.
[12] Q. Zhang and H. Li, MOEA/D: A multiobjective evolutionary algorithm based on de-composition, IEEE Trans. Evol. Comput., vol. 11, no. 6, pp. 712C731, Dec. 2007.
[13] Q. Zhang, W. Liu, E. Tsang, and B. Virginas, Expensive multiobjective optimization by MOEA/D with Gaussian process model, IEEE Trans. Evol. Comput., vol. 14, no. 3, pp. 456C474, Jun. 2010.
[14] E. Zitzler and S. Knzli, Indicator-based selection in multiobjective search, in Proc. Int. Conf. Parallel Prob. Solv. Nat., Birmingham, U.K., 2004, pp. 832C842.
[15] H. Trautmann, T. Wagner, and D. Brockhoff, R2-EMOA: Focused multiobjective search using R2-indicator-based selection, in Learning and Intelligent Optimization. Berlin, Germany: Springer, 2013, pp. 70C74.
[16] K Li, K Deb, Q Zhang, et al, "An Evolutionary Many-Objective Optimization Algo-rithm Based on Dominance and Decomposition," IEEE Transactions on Evolutionary Com-putation, 2015, 19(5):694-716.
[17] L. Ma, S.Cheng, X. Wang, M.Huang, H. Shen, X. He, Y. Shi. Co-operative Two-engine Multi-objective Bee Foraging Algorithm with Reinforcement Learning, Knowledge-Based Systems,133(2017):278-293,201.
[18] Zhang X, Tian Y, Jin Y. A Knee Point-Driven Evolutionary Algorithm for Many-Objective Optimization[J]. IEEE Transactions on Evolutionary Computation, 2015, 19(6):761-776.
[19] S. Bechikh, L. B. Said, and K. Ghdira, Searching for knee regions in multi-objective optimization using mobile reference points, in Proc. ACM Symp. Appl. Comput., Sierre, Switzerland, 2010, pp. 1118C1125.
[20] Vlachou A, Doulkeridis C, Kotidis Y. Angle-based space partitioning for efficient par-allel skyline computation[C]// ACM SIGMOD International Conference on Management of Data. ACM, 2008:227-23.